



HAL
open science

Aircraft trajectory prediction in North Atlantic Oceanic Airspace by Wind Networking

Olga Rodionova, Daniel Delahaye, Mohammed Sbihi, Marcel Mongeau

► **To cite this version:**

Olga Rodionova, Daniel Delahaye, Mohammed Sbihi, Marcel Mongeau. Aircraft trajectory prediction in North Atlantic Oceanic Airspace by Wind Networking. DASC 2014, 33rd Digital Avionics Systems Conference, Oct 2014, Colorado Springs, United States. hal-00996689

HAL Id: hal-00996689

<https://enac.hal.science/hal-00996689>

Submitted on 16 Oct 2015

HAL is a multi-disciplinary open access archive for the deposit and dissemination of scientific research documents, whether they are published or not. The documents may come from teaching and research institutions in France or abroad, or from public or private research centers.

L'archive ouverte pluridisciplinaire **HAL**, est destinée au dépôt et à la diffusion de documents scientifiques de niveau recherche, publiés ou non, émanant des établissements d'enseignement et de recherche français ou étrangers, des laboratoires publics ou privés.

TRAJECTORY PREDICTION IN NORTH ATLANTIC OCEANIC AIRSPACE BY WIND NETWORKING

Olga Rodionova, Daniel Delahaye, Mohamed Sbihi, Marcel Mongeau,

ENAC, MAIAA, F-31055 Toulouse, France and Univ de Toulouse, IMT, F-31400 Toulouse, France

Abstract

Aircraft in the North Atlantic oceanic airspace are subjected to strong winds caused by the Jet Stream. The flight progress prediction is based on meteorological data forecast. The roughness in wind forecast often results in large differences between the predicted and the actual cruising times. This increases the uncertainty in conflict detection. All aircraft are able to perform instant meteorological measurements. Implementing new technologies enables exchanging these measured data directly between aircraft. Thus, an aircraft can obtain information about winds on its route from preceding aircraft and adjust its time predictions. This process is called Wind Networking. As the data obtained with wind networking is much more accurate than the initial forecast, the adjusted predictions are much closer to the reality.

In this work, we perform simulations of the wind networking process. We compare the results of applying this approach and the results obtained using the meteorological forecast in terms of cruising time prediction and conflict prediction. We observe a remarkable improvement in the predictions by the wind networking and we quantify the benefits of using such an approach.

Introduction

The *North Atlantic oceanic airspace* (NAT) accommodates air traffic between two densely populated areas - North America and Europe. Aircraft crossing NAT are subjected to very strong winds caused by the presence of *Jet Streams* (JSs). JSs are fast narrow predominantly west-east air currents mainly located in the upper troposphere that are caused by a combination of the earth rotation and atmospheric heating (Figure 1). Two types of JSs are distinguished in NAT: *subtropical* JSs raised by the westerly acceleration of poleward moving air in the upper tropical circulation and *eddy-driven* JSs

provoked by the momentum and heat forcing from transient midlatitude eddies [1, 2]. The speed of the JS is typically 100 kts (nautical miles per hour) but can reach 200 kts.

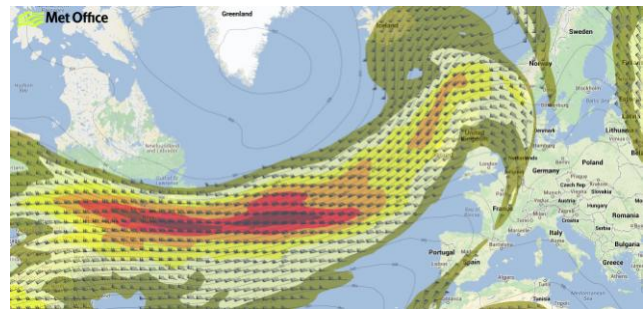


Figure 1. Jet Stream in NAT¹

Air traffic in NAT mainly contributes to two major flows: the westbound flow departing from Europe in the morning, and the eastbound flow departing from North America in the evening. Because of the time zone differences and passenger demands, these flows are separated in time. In the free flight conditions, the eastbound flights would try to exploit the JS in order to benefit from strong tailwinds, while the westbound flights would avoid the JS in order to minimize headwind [3]. As a result the two main flows are found to be separated in space as well; thus, they can be treated independently.

There are more than 500 flights crossing the NAT in each direction daily. As their wind-optimal routes are very close to each other, the NAT is highly congested at peak hours. Standard radar-based surveillance is not available for most part of this vast airspace. In order to increase efficiency of the Air Traffic Control (ATC) [4] and to perform conflict-free flight progress, the concept of parallel flight tracks known as the *Organized Track System* (OTS) was introduced in NAT [5]. Two independent OTS

¹ Met Office News Blog, <https://metofficenews.wordpress.com/tag/jet-stream/>

(RSS) should reach 2 minutes for consecutive aircraft on the same track, and 3 minutes for re-routing aircraft [6, 7]. Using the RSS raises significantly the NAT traffic accommodation capacity and the efficiency of individual flights by allowing the aircraft to follow more optimal routes [15, 16]. At the same time, it needs precise aircraft position determination and thus, more precise trajectory prediction.

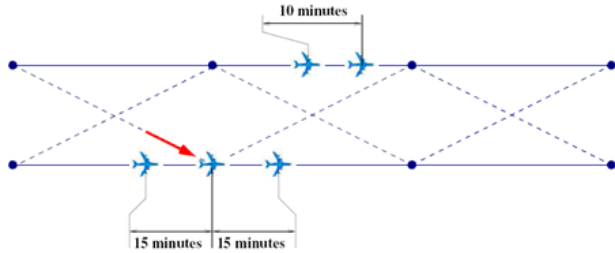


Figure 4. Longitudinal separation standards

Currently, the flight progress prediction relies on the *meteorological forecast* (MF) data (especially, wind maps). Typically MF data is not sufficiently precise [17-20] and yields substantial errors in aircraft trajectory predictions [21, 22]. This in turn increases the uncertainty in conflict detection and the difficulty of tactical conflict resolution. At the same time, all aircraft are supplied with equipment capable to perform instant meteorological measurements (temperature, pressure, wind speed) during the flight [23-25]. Even though such measurements are always carried out with some inaccuracy [26-28], having the possibility to use them in wind forecast adjustment can significantly improve flight predictions [29, 30].

New surveillance and broadcast services (ADS-B, Flight Information Services-Broadcast (FIS-B) [31, 32]) allow aircraft to exchange the measured meteorological data with the ground ATC and with each other directly en-route (Figure 5). Thus, an aircraft can obtain recent and more precise information about winds on its route from preceding aircraft, and can update its time predictions based on these data. We call this process: *Wind Networking* (WN).

The current work is devoted to evolve and quantify the benefits of using WN approach in aircraft trajectory prediction and conflict detection. First we describe the modeling of the NAT air traffic situation. Next we discuss more precisely the WN

approach. Finally, the simulation results are presented followed by the comparison of the two prediction methods: MF and WN.

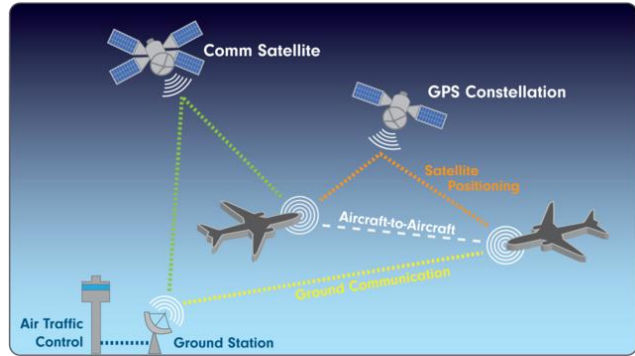


Figure 5. New surveillance/broadcast services [31]

NAT air traffic models

This section describes the models we propose for the NAT air traffic simulations: wind model, OTS model and flight model. Further modeling of the real flight progress and its prediction using the MF is introduced. In this work, we focus on simulating the NAT eastbound traffic. Westbound traffic can be treated in the same manner.

Wind model

The quality of aircraft trajectory prediction depends first of all on the quality of wind prediction. To evaluate the prediction accuracy, one needs to compare the predicted wind values with the real ones. The difficulty is that the real wind is actually unknown. The forecast wind can be obtained from meteorological databases. Thus, a large amount of works devoted to modeling wind for aviation focus on modeling the deviations of the predicted wind from the real one [20, 33, 34]. These deviations are generally given under statistical form [17, 35] that requires adjusting several parameters. As to our knowledge there was no precise study similar to [29] determining the statistical parameters for NAT, we propose another approach to model both real and forecast winds, and their deviation.

We rely on the GRIB data files created by the meteorological centers (NOAA, Meteoblue, FNMOC), which are available online [36]. A GRIB file consists of several grids coded in a special format

[37]. Each such grid represents a regular grid of geographical points with maximal resolution of 0.5° , where various MF data is defined for each point. We study the area from 35°N to 70°N of latitude and from 0°W to 75°W of longitude, which covers the NAT. We extract only the u (west-east) and v (north-south) wind components for each point. Each grid is defined for a specific time for which the MF is valid (with 3-hour time step) and for a specific altitude. We concentrate on the time period from 0000 UTC to 0900 UTC that includes the eastbound OTS validity period, and on the altitudes 300hPa and 200hPa that bound the published OTS FLs. We decode the GRIB files with the open-source java library JGrib [38].

In order to simulate one day of traffic, we rely on two GRIB files downloaded with time difference of several (from 18 to 24) hours. We use the data from the first (the oldest) file as forecast winds. The second (the latest) file is used to model the real winds, as its data is more recent and therefore tends to represent better the reality. Figure 6 displays the wind fields obtained from the two GRIB files available for 10 December 2013 at the altitude 200 hPa. The left column corresponds to the forecast wind; the right column simulates the assumed real wind. Two time moments: 0000 UTC (upper line) and 0600 UTC (lower line) are considered in this example to illustrate the wind evolution. As it can be seen from Figure 6, the forecast and real wind fields differ slightly.

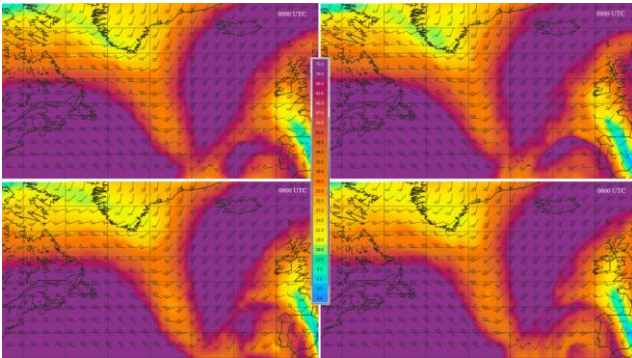


Figure 6. Forecast and real wind fields

GRIB files only provide information about the winds at discrete grid points. We obtain the continuous wind fields by linear interpolation over grids in 4-dimensional space (time, altitude, latitude and longitude). With current grid resolution the 4D linear interpolation coincides satisfactorily with the

reality. Remark that most wind models also rely on such an approach.

OTS model

As the OTS is constructed daily based on the wind fields, it is important to use wind forecast and OTS valid corresponding to the same day in the simulations. The current [39] and the archived [40] OTS can be found online in free access in the form of NAT messages. Such messages contain a number of OTS tracks defined for a particular day, where each track is represented by a sequence of WPs followed by a sequence of FLs available for the current track. Figure 7 displays the eastbound OTS defined on 10 December 2013 projected on the horizontal plane.

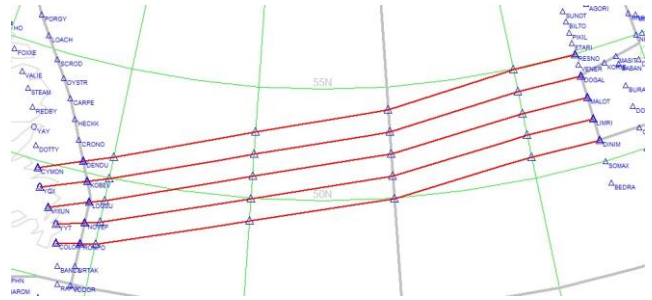


Figure 7. Eastbound OTS on 10 December 2013

We propose to model an OTS with a $N_x \times N_y \times N_z$ grid of WPs, where N_y is the number of OTS tracks, N_x is the number of WPs on each track, and N_z is the number of FLs for each track. The tracks are labeled from 1 to N_y starting from the most northern, the WPs on each track from 1 to N_x starting from the most western, and the FLs from 1 to N_z starting from the lowest. Thus, the 3D position of an aircraft on track j at WP i at FL k is completely specified by the vector (i, j, k) . The geographical coordinates of this point are given by the vector $(\lambda_i^j, \varphi_i^j, h_k)$, where λ_i^j is the point longitude, φ_i^j is the point latitude and h_k is the point altitude.

Every pair of consecutive WPs on the same track: (i, j, k) and $(i + 1, j, k)$ are joined with straight lines called *links*. Similarly, every pair of consecutive WPs on adjacent tracks, northern: (i, j, k) and $(i + 1, j - 1, k)$; southern: (i, j, k) and $(i + 1, j + 1, k)$, are joint with links. Thus, each WP (except for those

on the outer tracks) has three outgoing links. We call the link intersection points as *nodes*. Figure 8 displays the horizontal section of our OTS model represented by a grid of nodes joined with links. In addition to WPs that are located on tracks and that belong to the OTS grid structure (red nodes in Figure 8) the node set also contains the points of intersection of the links joining adjacent tracks (blue nodes in Figure 8).

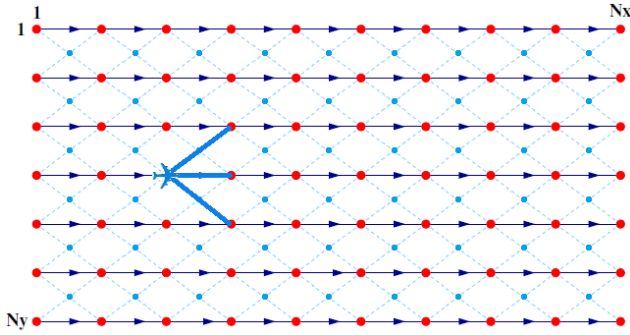


Figure 8. OTS model (horizontal section)

Flight model

We considered several flight sets with various numbers of flights in our simulations. For some tests the flight input parameters were set randomly (respecting both the ATC regulations and our model constraints). Other tests were performed using real flight sets extracted from the FPL (flight plan) messages. Such messages are available for several days of August 2006 from the ASSTAR project [6] (we did not have the access to more recent data).

Here is how we simulate the flight progress of N aircraft crossing the NAT within the OTS. For each flight f we define the entry (Tr_{in}^f) and exit (Tr_{out}^f) tracks, and the track entry time (t_{in}^f). If the entry and exit tracks are different, we choose the WPs where the aircraft performs re-routings. Thus, the aircraft route between the entry and exit WPs consists of a sequence of links. We limit our model to authorize only re-routings towards the exit tracks in order to avoid north-south zigzagging.

We assume that while moving along a link, an aircraft maintains constant air speed (Mach number) and constant FL. Thus, true air speed (v_i^f) and FL

(FL_i^f) are to be set only at WPs ($i=1, \dots, Nx$). Furthermore, we assume that the speed difference between two consecutive WPs (i and $i+1$) does not exceed 0.02 Mach. Current practice tends to show that the FLs difference is very rarely above 2 FLs [8]. In addition to this, aircraft are allowed only to climb (not to descend), in order to satisfy the optimal kerosene consumption flight profile. Figure 9 displays the vertical section of the OTS grid and shows possible altitude profiles for eastbound flights. In our model, the distance between the real horizontal position of the aircraft at the new FL and the previous WP after climbing (see Figure 9) is neglected, as well as the time required to reach the new FL. This instantaneous-climbing hypothesis is reasonable, as the distance between the WPs (10° of longitude, or about 500 km) is much longer than the vertical distance between FLs (1000 feet, or 0.3048 km).

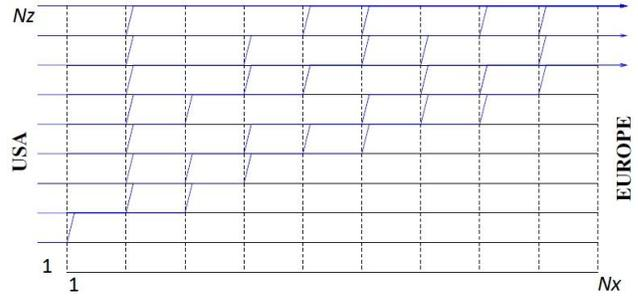


Figure 9. OTS model (vertical section)

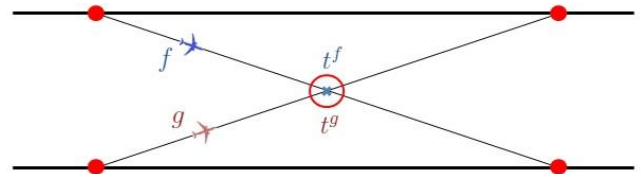


Figure 10. Conflict at a common route node

The particularity of our OTS model imposes that the flight interactions can only happen on links or at nodes. Lateral and vertical separation being ensured by the OTS construction, a conflict may only occur when a longitudinal separation constraint is violated for a pair of consecutive flights. A conflict can occur on a link if one aircraft is slower than the other following it on the same track. A conflict is detected on a node (shown with a red circle in Figure 10) when two consecutive aircraft pass this node with a time difference violating the longitudinal time separation minimum. The task of ATC is to detect

and eliminate such conflicts (see [16]). In the current paper we focus only on conflict detection and on the comparison of prediction methods.

Flight progress simulation and prediction

To simulate flight progress within NAT, we need to compute for each aircraft the times of passing the route points. These times are computed based on the aircraft ground speed. While the aircraft true air speed is a given parameter for a segment of flight, the ground speed varies according to the wind that the aircraft is subjected to.

Let us consider an aircraft f moving at FL k from WP i on track j towards the next WP $i+1$ on track j' (where $j' = j, j' = j-1$ or $j' = j+1$) along the corresponding link (Figure 11). Let us assume that at the time t this aircraft is located at the point with coordinates (λ, φ, h_k) . Its air speed is equal to v_i^f at this point (black arrow in Figure 11). The *real wind speed* at this point is equal to $\vec{W}(t, \lambda, \varphi, h_k)$ (blue arrow in Figure 11). Then, its real ground speed V^f (red arrow in Figure 11) is defined by the formula:

$$V^f = v_i^f + W_{ijj'}(t, \lambda, \varphi, h_k), \quad (1)$$

where $W_{ijj'}(t, \lambda, \varphi, h_k)$ is the projection of the wind vector on the link $(i, j, k) - (i+1, j', k)$.

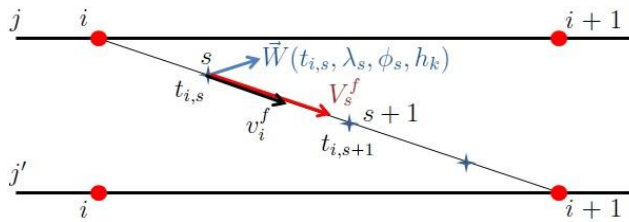


Figure 11. Simulation of flight between two WPs

Given the time t_i at which aircraft f was at the WP (i, j, k) , we are interested to compute the time t_{i+1} at which this aircraft arrives at the WP $(i+1, j', k)$. To compute this time, we divide the corresponding link $(i, j, k) - (i+1, j', k)$ into N_f sublinks and obtain $N_f + 1$ subnodes (marked with

stars in Figure 11). The ground speed V_s^f at each subnode $s=1, \dots, N_f + 1$ can be calculated via formula (1). To simplify the simulation, we suppose that this speed remains constant and equal to V_s^f along the link segment between subnodes s and $s+1$. Let us denote the length of this link segment as l_s . Then, the time $\Delta t_{i,s}^f$ necessary for aircraft f to move from subnode s to subnode $s+1$ is simply:

$$\Delta t_{i,s}^f = \frac{l_s}{V_s^f}. \quad (2)$$

Using these time periods $\Delta t_{i,s}^f$ and given the link entry time t_i^f (which is the time of passing the first subnode, $t_{i,1}^f = t_i^f$), the times $t_{i,s}^f$ at which aircraft f passes subnodes s can be successively calculated for $s=2, \dots, N_f + 1$:

$$t_{i,s}^f = t_{i,s-1}^f + \Delta t_{i,s-1}^f. \quad (3)$$

We thereby obtain all the necessary information to perform the simulation of aircraft flight along any link (and for the whole OTS). Note that $t_{i,s}^f$ is the *real (actual) time* of arrival of aircraft f at subnode s . In addition, we consider the *forecast times*, noted as $\tilde{t}_{i,s}^f$, *i.e.* the times at which the aircraft estimates to be at subnode s using the available MF information. This time is supposed to be different from the actual time, as the exact values of real oceanic winds are not known. The *forecast times* $\tilde{t}_{i,s}^f$ can be calculated based on the *forecast wind function* $\vec{W}^{\sim}(t, \lambda, \varphi, h_k)$ using formulas analogous to (1)-(3). Figure 12 displays the differences between real and forecast flight values. The aircraft air speed v_i^f is represented with black arrow, the *real wind speed* \vec{W} with blue arrow, while the *forecast wind speed* \vec{W}^{\sim} , slightly different, with green arrow. Thus, the *forecast ground speed* \tilde{V}^f (violet arrow) also differs from the *real ground speed* V^f (red arrow).

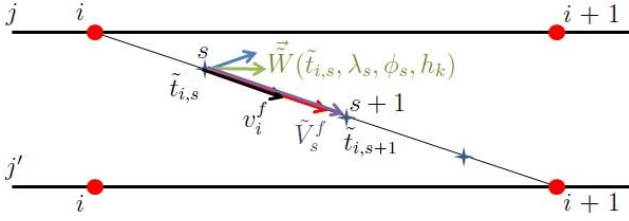


Figure 12. Estimation of flight between two WPs

Wind Networking approach

This section describes the main idea of the WN approach. It explains how the approach was implemented in our simulations. Finally, it presents the criteria to be used for evaluating the WN benefits.

Wind Networking simulation

Let us suppose that aircraft f on route passing the point (λ, φ, h_k) at time t^f can measure the wind $\vec{W}(t^f, \lambda, \varphi, h_k)$ at this point (dark blue arrow in Figure 13, top). Measurements are assumed to be performed with some error $\vec{\delta}^f$. Thus, instead of the real wind function the aircraft obtains its approximation (light blue arrow in Figure 13):

$$\vec{W}^f(t^f, \lambda, \varphi, h_k) = \vec{W}(t^f, \lambda, \varphi, h_k) + \vec{\delta}^f. \quad (4)$$

In our simulations the measurement error $\vec{\delta}^f$ is assumed to be normally distributed, $\vec{\delta}^f \sim N(0, \sigma)$ with mean equal to 0 and standard deviation $\sigma = 1.1$ m/s. The value of σ is set according to the statistics obtained from the previous studies [26, 29].

Further, we suppose that aircraft can communicate the results of these measurements to other aircraft (see Figure 13, bottom). Based on the information about the winds received from preceding aircraft, the following aircraft (g , shown in red in Figure 13) can *adjust* its predictions. This information (\vec{W} , red arrow in Figure 13) is expected to be more precise than MF winds (\vec{W} , green arrow in Figure 13), as it is more recent. Thus, the *adjusted predictions* should be closer to the real situation than the initial forecast. That is the main idea of WN.

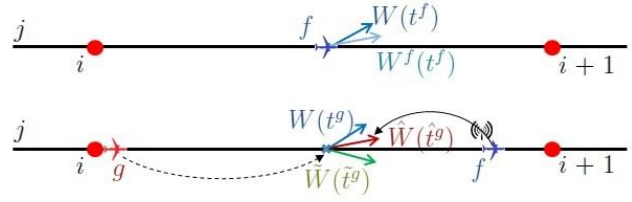


Figure 13. Adjusting wind predictions by WN

Let us consider that aircraft f moves at FL k , from WP i on track j towards the next WP $i+1$ on track j' along the corresponding link. Being at the WP i at time t_i^f the aircraft needs to predict its flight until WP $i+1$. To simulate this process, we divide again the link $(i, j, k) - (i+1, j', k)$ into N_f sublinks. Using the forecast wind field \vec{W} , we obtain the forecast times of passing the subnodes: $\tilde{t}_{i,s}^f$, $s = 1, \dots, N_f + 1$. Here is how we propose to improve these predictions using the WN approach.

Let us consider m aircraft f_1, f_2, \dots, f_m on the OTS on the links *neighbor* to the link $(i, j, k) - (i+1, j', k)$ that passed the corresponding links before the aircraft f (before $t_{i,s}^f$). The choice of the links, that are considered to be *neighbor* to the current one, can vary according to user preferences. The set of neighbor links may include the current link itself, several upper/lower links and/or several northern/southern links. Here is how we define the neighbor links for most of the simulations. Let us denote $j_{\min} = \min(j, j')$ and $j_{\max} = \max(j, j')$. Then, the neighbors of the link $(i, j, k) - (i+1, j', k)$ in horizontal plane (on FL k) are all possible links between WPs i and WPs $i+1$ on the tracks $j_{\min} - 1, j_{\min}, j_{\max}, j_{\max} + 1$. Figure 14 displays one example of determining all neighbor aircraft (blue) of aircraft f (red) in the horizontal section of the OTS. In the vertical direction we consider only the 2 links on the adjacent FLs – upper and lower, *i.e.* the links $(i, j, k+1) - (i+1, j', k+1)$ and $(i, j, k-1) - (i+1, j', k-1)$.

Aircraft f then can use the wind measurements from preceding aircraft f_1, \dots, f_m in the prediction of

its flight. Considering that each such aircraft f_n measured $N_{f_n} + 1$ winds on the corresponding link, we obtain the following wind data available for aircraft f :

$$\vec{W}^{f_n} \left(t_{s_n}^{f_n}, \lambda_{s_n}, \varphi_{s_n}, h_{k_n} \right), \quad (5)$$

where $n=1, \dots, m$ is the index of preceding aircraft, $s_n=1, \dots, N_{f_n} + 1$ is the index of subnode on the link followed by this aircraft with the coordinates $(\lambda_{s_n}, \varphi_{s_n}, h_{k_n})$, $t_{s_n}^{f_n}$ is the time of passing of this subnode by the aircraft f_n and \vec{W}^{f_n} is the wind, measured by this aircraft at this moment (blue arrows in Figure 14).

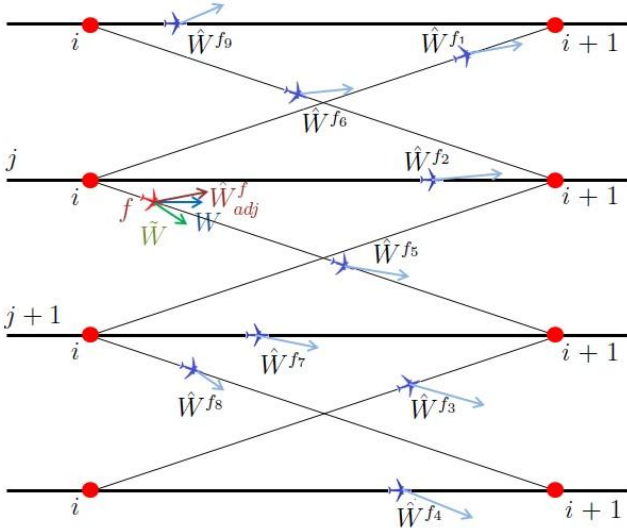


Figure 14. Adjusting wind predictions by WN

Further, we can apply any appropriate extrapolation method to the corresponding measurements (5) in order to obtain the adjusted wind at each subnode $s=1, \dots, N_f + 1$ on the route link of aircraft f : $\vec{W}_{adj}^f \left(\hat{t}_{i,s}^f, \lambda_s, \varphi_s, h_k \right)$. Here $\hat{t}_{i,s}^f$ is the aircraft predicted *adjusted time* of passing the subnode s , that can be calculated using formulas similar to (1)-(3). The adjusted wind \vec{W}_{adj}^f is shown with red arrow in Figure 14 and it is supposed to be closer to the real wind (blue arrow) than the forecast wind (green arrow) at the same point.

Wind Networking evaluation criteria

The main objective of this study is to evaluate the quality of the two prediction approaches: using MF and WN. The first criterion of comparison is the error made in the time prediction. To measure these errors, we compute for each flight f and for each WP i of its route the difference between the real and the predicted times of arrival at this WP:

- $\tilde{e}_i^f = \tilde{t}_i^f - t_i^f$ for forecast times;
- $\hat{e}_i^f = \hat{t}_i^f - t_i^f$ for adjusted times,

and we analyze and compare the prediction errors (\tilde{e}_i^f and \hat{e}_i^f) distributions.

Another criterion of comparison is the number of conflicts detected for the set of flights using each of the prediction approaches:

- the number of conflicts that are predicted (by each of the method) but do not happen in the reality (*false alarms*);
- the number of conflicts that would happen but have not been predicted (*critical errors*);
- the errors in the conflict duration predictions (related to the time prediction errors).

The results of these comparisons are presented in the next section.

Simulation results

Several days of the years 2013-2014 were analyzed during this study. Here we present the results of simulations for 10 December 2013. The results for the other days are similar. The real and forecast wind fields used for this day are shown in Figure 6, and the valid eastbound OTS is displayed in Figure 7. Remark that the OTS passes through the area of very strong winds, which increases the uncertainty in the aircraft position determination.

Results for one track

Our first preliminary study considers a simple model consisting of several consecutive flights

following one track on the same FL. For this model, several first aircraft enter every link without having preceding aircraft that already past the corresponding link, and thus, they cannot benefit from the WN approach. On the other hand, the rest of aircraft obtain complete information about the winds from all preceding aircraft for each route point. This case could very rarely happen in the reality, but it demonstrates the benefits of the WN approach under ideal conditions.

Several tests, hold with different extrapolation methods for adjusting the wind for the particular aircraft from the measurement of the preceding aircraft, revealed that using data from the latest available aircraft for the adjusted wind yields results that are as good as (and in some cases, even much better then) when applying any extrapolation method to wind values obtained from several aircraft. Thus, we focus only on these last-aircraft results in this paper.

In the example below, we consider a flight set consisting of 77 aircraft cruising on the middle OTS track (VIXUN-MALOT) at the altitude 200hPa. The flight track entry times were randomly chosen between 0000 UTC and 0500 UTC so that all aircraft exited the OTS before 0900 UTC and were separated by at least 3 minutes (according to RSS) throughout the track. First, we perform the flight simulations using the real wind field, next using the forecast wind, and finally using the wind obtained from the latest previous aircraft. For this example, the first 10 aircraft were too close one to each other to provide sufficient information (for all subnodes on links) to the following aircraft. Thus, the WN approach was only applied to the rest 67 aircraft. For each simulation, we recorded the times of passing the WPs: t_i^f , \tilde{t}_i^f and \hat{t}_i^f . Then, for the two prediction approaches, we calculated the prediction errors at each WP, i.e. \tilde{e}_i^f and \hat{e}_i^f . Figure 15 shows the two prediction-error distributions obtained. The time scale in this diagram was truncated to 30 seconds in order to focus on the mean error values.

Table 1 presents some statistics of the distributions of prediction-error absolute values. As it can be seen from this table and from Figure 15, the WN approach improves significantly the prediction of the time of passing the WPs. The average

prediction error from almost half a minute (an important value for RSS) is reduced to less than 5 seconds. These encouraging results of WN application obtained for this artificial flight model give the stimulus to apply the approach to the real air traffic in NAT.

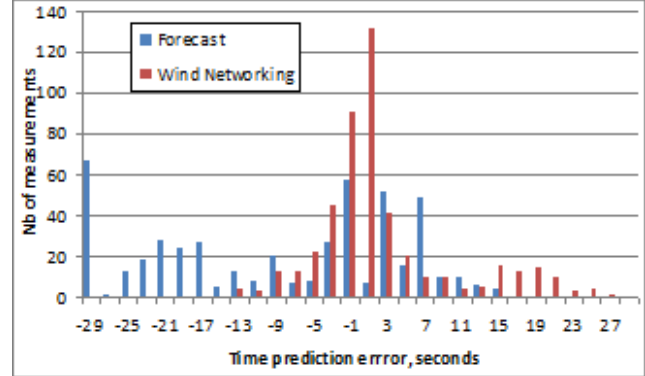


Figure 15. MF vs. WN prediction error, 77 flights

Table 1. Prediction error statistics, 77 flights

Approach	MF	WN
Value (sec.)	$ \tilde{e}_i^f $	$ \hat{e}_i^f $
Max	215,61	26,97
Mean	29,67	4,86
Variance	50,83	6,04

Results for real aircraft set on OTS

On the next step of our research we apply the WN approach to real air traffic data. Several data sets have been tested. In the example below we consider a set of 378 aircraft cruising between 38 airports in North America to 51 airports in Eurasia (mostly in Europe) for 4 August 2006. In order to reduce the congestion in the continental airspace, the desired entry track is assumed to be the track that is the closest to the departure airport, and similarly for the desired exit track (closest to the arrival airport) (see [16] for more detail). The desired track entry time is first set to be the same as defined in the flight plan, and then it is adjusted in order to fit into the range of the OTS validity (starting from 0000 UTC). Finally, the flights are reorganized in order to avoid conflicts on links (when faster aircraft overcome

slower ones), so that all remaining conflicts are conflicts on nodes.

The constructed flight set is evaluated using three different winds and the errors of time prediction of passing the WPs are compared. We have tested several extrapolation approaches to obtain the adjusted wind from neighbor preceding aircraft. Figure 16 displays the prediction error distributions for some of these approaches, *i.e.* when:

- only the measurements received from the latest aircraft on the same link are taken into account (as in the previous subsection) (blue in Figure 16);
- the wind values obtained from the closest (in terms of distance) aircraft on the neighbor links are linearly interpolated to adjust the wind at the current aircraft position (red in Figure 16);
- the wind values obtained from the latest (in terms of time) aircraft on the neighbor links are linearly interpolated (green in Figure 16).

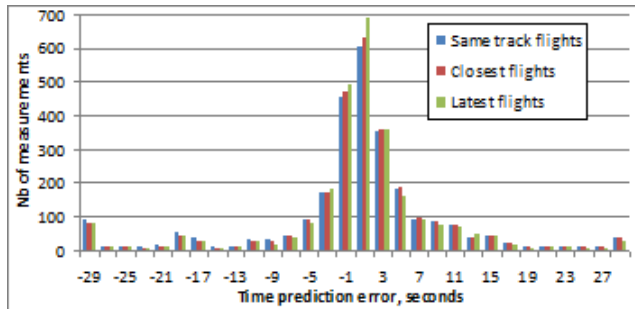


Figure 16. Wind extrapolation comparison

Table 2. Prediction error statistics, 378 flights

Approach	MF	WN, same track	WN, closest	WN, latest
Mean, sec	16.36	7.48	6.87	6.40
Var., sec	22.05	13.51	12.53	12.21

The statistics of the distributions of the absolute values of these prediction errors are presented in Table 2. This table and Figure 16 show that using the measurements from aircraft on neighbor links

improves the results; and the more recent the measurements are, the smaller the prediction errors are, and the closer to the reality the results are. Thus, in the sequel of this paper the WN approach always refers to the method based on the measurements from the most recent (latest in time) neighbor aircraft.

Figure 17 presents the comparison of the distributions of the prediction errors using MF approach (its statistics can be found in Table 2 as well) and WN approach (based on the best “latest flights” extrapolation method); the bottom diagram displays a truncated time scale in order to better demonstrate the distribution behavior near 0.

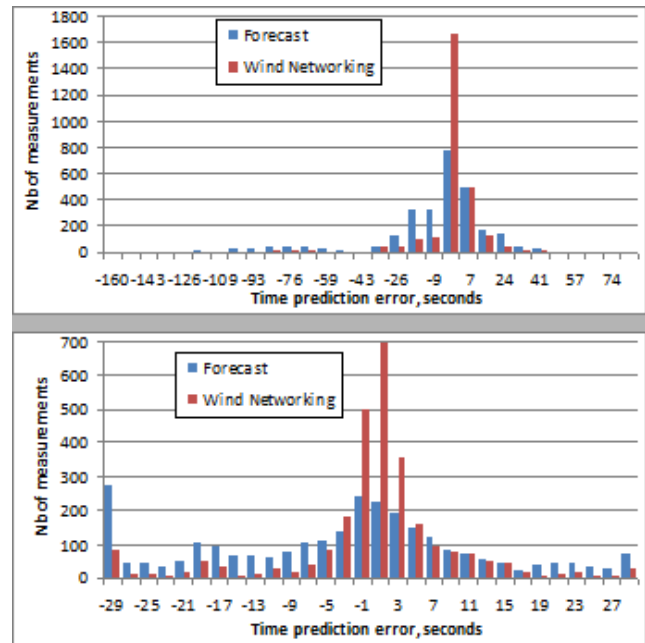


Figure 17. MF vs. WN prediction error, 378 flights

Comparison of the results from this subsection (Figure 17) with the previous results (Figure 15) shows that the WN approach seems to be less efficient in the case of several tracks and real aircraft sets: the prediction error being less than 5 seconds for one-track artificial flight set grows up to 7 seconds in the real case. Here are some explanations of this phenomenon:

- the difference in the wind evaluation for different tracks (WN is more efficient if the wind does not change much with the time);

- the time period between the consecutive flights (WN is more efficient if this period is short, which was the case for artificial flight set, but not always the case for the real one);
- the existence of previous flights (for the artificial flight set, all flights followed one another; in the real case, some flights on some links may have no preceding flights; this obliges such flights to rely on MF instead of WN, and thus, the predictions are not improved at all).

On the next stage of prediction method comparison, we concentrate on evaluating the error in conflict prediction. As mentioned above, conflicts can only happen on nodes in the considered model. First of all, we perform the flight simulation based on the three wind functions and we record the pairs of aircraft in conflict (violating longitudinal separation minimum) at each OTS node. Then, we compare the real situation with each of the prediction methods to determine the number of conflicts that were predicted correctly, the number of false alarms, and the number of critical errors. The first three lines of Table 3 display these numbers.

Table 3. Conflict prediction, 378 flights

Approach	MF	WN
Correctly predicted, Nb.	460	462
False alarms, Nb.	11	7
Critical errors, Nb.	12	10
Conflict duration error, minutes	46,29	21,63

The last line of Table 3 contains the absolute value of the total conflict duration time error (which is the difference between the predicted conflict duration time and the real one, considering that if the conflict is not detected its duration is 0). Figure 18 represents the distributions of conflict duration errors for both prediction approaches. The scale is truncated at 30 seconds in order to visualize better the distribution near its mean value.

Table 3 and Figure 18 reveal the improvement in conflict prediction when using the WN approach. Obviously, this improvement is directly related with

the accuracy of the approach in time prediction. It seems quite reasonable that the more aircraft there are the greater improvement could be achieved using WN, as more aircraft would benefit from the measurements of preceding aircraft. This hypothesis becomes even more important once remembering that the number of flights in airspace is constantly increasing. This fact encourages performing the simulations for artificially increased flight sets.

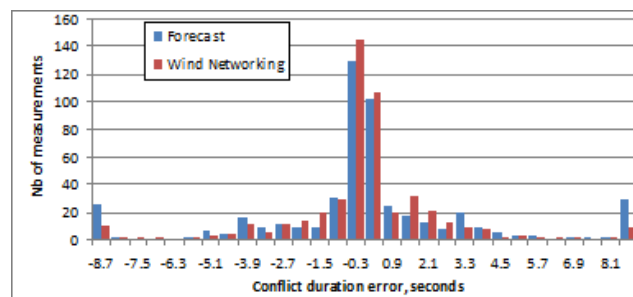


Figure 18. Conflict duration error, 378 flights

Results for increased flight set on OTS

In this subsection we present the results similar to those discussed in the previous section but for an increased flight set. In the example below we consider 1000 flights. As in any case such a flight set would be an artificial one, we chose the desired entry and exit track as well as the desired track entry time randomly. Further, these parameters were adjusted in order to eliminate the conflicts on links. We perform the simulations in the same manner as it was described in the previous subsection: we compute the prediction errors of time of passing the WPs for both approaches, the number of correctly and incorrectly predicted conflicts, the errors in conflict duration prediction.

Figure 19 presents the distribution of time prediction errors (the time scale is truncated at 1 minute). The mean absolute value of MF error in this case is 22.35 seconds; and the mean absolute value of WN error is 5.83 seconds. One can again notice the improvement in WP passing times predictions using the WN that is even greater for this case of 1000 flights in comparison to real 378 flights.

Table 4 contains the number of correctly predicted conflicts, the number of false alarms and the number of critical errors, as well as the total absolute value of conflict duration prediction errors.

What is remarkable, in this case the numbers of incorrect conflict predictions as well as the conflict duration errors in average are reduced almost in 4 times when applying the WN.

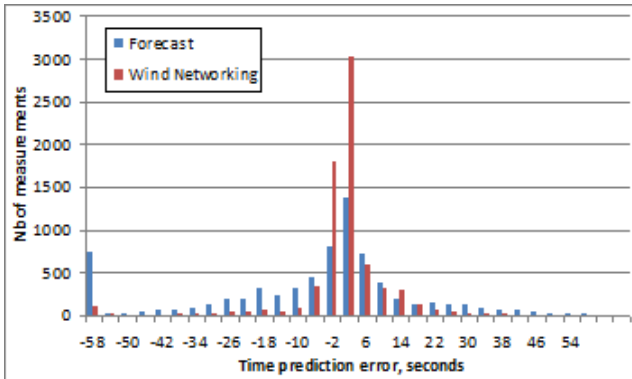


Figure 19. MF vs. WN prediction error, 1000 flights

Table 4. Conflict prediction, 1000 flights

Approach	MF	WN
Correctly predicted, Nb.	1175	1229
False alarms, Nb.	48	13
Critical errors, Nb.	70	16
Conflict duration error, min.	242.7	63.4

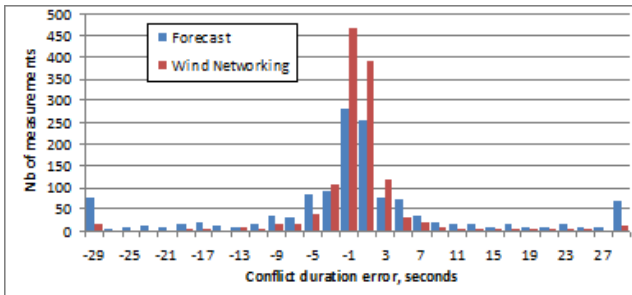


Figure 20. Conflict duration error, 1000 flights

When observing the conflict duration prediction errors distribution (see Figure 20) one can also easily notice much greater improvement due to WN in comparison to real flight set (Figure 18). This fact reveals the absolute benefits of WN approach especially for dense traffic conditions.

Conclusion

The current paper introduces the Wind Networking approach for aircraft trajectory prediction in North Atlantic oceanic airspace. The approach is based on the possibility to use measurements from previous aircraft to adjust the forecast wind.

The paper describes the mathematical model based on which the numerical simulations were held on. During the simulations several days with different meteorological conditions were studied. The paper presents the results for one day and several flight sets that were found to be quite typical.

The results of the simulations reveal the significant decrease in the errors of prediction of times of passing the waypoints for the set of aircraft in average when applying WN approach. They also show that the number of en-route conflicts as well as their duration time are also predicted much more precisely using WN. Finally, the study performed for increased flight sets prove the special efficiency of WN in the dense traffic conditions.

Thus, the WN seems to be a very promising approach to improve the flight trajectory prediction, which is especially important in oceanic airspace because of the lack of surveillance abilities. Implementing of this approach that would be possible due to new broadcast technologies will allow aircraft to know their future position in time more exactly and to determine possible conflicts more precisely in order to efficiently avoid them.

The WN brings improvement in particular in dense areas. Those areas are also the ones where a good trajectory prediction is critical. We expect in some future works to estimate the benefits of this concept in some other dense areas, like big terminal maneuvering areas.

References

[1] T. Woollings, A. Hannachi, B. Hoskins, 2010, Variability of the North Atlantic eddy-driven jet stream, Quarterly Journal of the Royal Meteorological Society, vol. 136, part B, pp. 856–868.

- [2] E. Gerber, G. Vallis, 2009, On the zonal structure of the North Atlantic oscillation and annular modes, *Journal of the Atmospheric Sciences*, vol. 66, pp. 332–352.
- [3] E. Irvine, B. Hoskins, K. Shine, R. Lunn, C. Froemming, 2013, Characterizing North Atlantic weather patterns for climate-optimal aircraft routing, *Meteorological Applications*, vol. 20, no. 1, pp. 80–93.
- [4] Y. Wu, L. Hamrick, T. Karakis, M. Merkle, 2004, Performance metrics for oceanic air traffic management, *Air Traffic Control Quarterly*, vol. 12, no. 4, pp. 315–338.
- [5] NAT Doc 007, 2012, Guidance concerning air navigation in and above the North Atlantic MNPS airspace, 2012th ed., International Civil Aviation Organisation, published on behalf of the North Atlantic Systems Planning Group (NAT SPG) by the European and North Atlantic Office of ICAO.
- [6] P. Louyot, 2007, ASEP-ITM simulations from traffic data, DSN, ASSTAR, WP8, Tech. Rep.
- [7] O. Rodionova, M. Sbihi, D. Delahaye, M. Mongeau, Optimization of aircraft trajectories in North Atlantic oceanic airspace, 5th International Conference on Research in Air Transportation - ICRAT 2012, Berkeley, CA.
- [8] Doc4444, 2007, Air Traffic Management, 15th ed., International Civil Aviation Organisation.
- [9] J. McHale, 2011, NextGen air traffic control avionics are moving from concept to cockpit, *Avionics Intelligence*, online articles.
- [10] J. McHale, 2010, ADS-B in enhances ATM and pilot situational awareness, *Avionics Intelligence*, online articles.
- [11] T. Cho, I. Song, E. Jang, W. Yoon, S. Choi, 2012, The improvement of aircraft position information with the unscented Kalman filter, *International Journal of Database Theory and Application*, vol. 5, no. 2.
- [12] L. Peng, Y. Lin, 2010, Study on the model for horizontal escape maneuvers in TCAS, *IEEE Transactions on Intelligent Transportation Systems*, vol. 11, no. 2, pp. 392–398.
- [13] M. Prandini, L. Piroddi, S. Puechmorel, S.L. Brazdilova, 2011, Toward air traffic complexity assessment in new generation air traffic management systems, *IEEE Transactions on Intelligent Transportation Systems*, vol. 12, no. 3, pp. 809–818.
- [14] P. Massoglia, M. Pozesky, G. Germana, 1989, The use of satellite technology for oceanic air traffic control, *Proceedings of the IEEE*, vol. 77, no. 11.
- [15] A. Williams, I. Greenfeld, 2006, Benefits assessment of reduced separations in North Atlantic Organized Track System, 6th AIAA Aviation Technology, Integration and Operations Conference (ATIO), Wichita, KS.
- [16] O. Rodionova, M. Sbihi, D. Delahaye, M. Mongeau, 2014, North Atlantic Aircraft Trajectory Optimization. *IEEE Transactions on Intelligent Transportation Systems*. To appear.
- [17] A. Hollingsworth, P. Lonnberg, 1986, The statistical structure of shortrange forecast errors as determined from radiosonde data. Part I: The wind field, *Tellus*, vol. 38A, no. 2, pp. 111–136.
- [18] B. Schwartz, S. Benjamin, S. Green, M. Jardin, 2000, Accuracy of RUC-1 and RUC-2 wind and aircraft trajectory forecasts by comparison with ACARS observations, *Weather and Forecasting*, vol. 15, pp. 313–326.
- [19] C. Cardinali, L. Rukhovets, J. Tenenbaum, 2004, Jet stream analysis and forecast errors using GADS aircraft observations in the DAO, ECMWF, and NCEP models, *Monthly Weather Review*, vol. 132, pp. 764–779.
- [20] S. Mondoloni, 2006, Aircraft trajectory prediction errors: Including a summary of error sources and data, FAA/Eurocontrol Action Plan 16, Tech. Rep. 2.
- [21] The International Federation of Air Line Pilots Associations IFALPA, 2011, Navigational errors on the North Atlantic, the Global Voice of Pilots, *Safety Bulletin*.
- [22] A. Lee, S. Weygandt, B. Schwartz, J. Murphy, 2009, Performance of trajectory models with wind uncertainty, AIAA Modeling and Simulation Technologies Conference, Chicago, IL.

- [23] R. Wood, 1997, Aircraft observations of boundary layer structure, Ph.D. dissertation, The University of Manchester Institute of Science and Technology.
- [24] D. Khelif, S. Burns, C. Friehe, 1999, Improved wind measurements on research aircraft, *Journal of Atmospheric and Oceanic Technology*, vol. 16, pp. 860–875.
- [25] W. Moninger, R. Mamrosh, P. Pauley, 2003, Automated meteorological reports from commercial aircraft, *Bulletin, American Meteorological Society*, vol. 84, pp. 203–216.
- [26] S. Benjamin, B. Schwartz, R. Cole, 1999, Accuracy of ACARS wind and temperature observations determined by collocation, *Weather and Forecasting*, vol. 14, pp. 1032–1038.
- [27] C. Drue, W. Frey, A. Hoff, T. Hauf, 2008, Aircraft type-specific errors in AMDAR weather reports from commercial aircraft, *Quarterly Journal of the Royal Meteorological Society*, vol. 134, pp. 229–239.
- [28] W. Moninger, S. Benjamin, B. Jamison, T. Schlatter, T. Smith, E. Szoke, 2010, Evaluation of regional aircraft observations using TAMDAR, *Weather and Forecasting*, vol. 25, pp. 627–645.
- [29] R. Cole, C. Richard, S. Kim, D. Bailey, 1998, An assessment of the 60km Rapid Update Cycle (RUC) with near real time aircraft reports, Lincoln Laboratory, Massachusetts Institute of Technology, project Report NASA/A-1.
- [30] R. Cole, S. Green, M. Jardin, 2000, Improving RUC-1 wind estimates by incorporating near-real-time aircraft reports, *Weather and Forecasting*, vol. 15, pp. 447–460.
- [31] J. Zimmerman, 2013, ADS-B 101: what it is and why you should care, *Air Facts*, the journal for personal air travel - by pilots, for pilots.
- [32] T. Gilbert, R. Bruno, 2009, Surveillance and broadcast services - an effective nationwide solution, *Integrated Communications, Navigation and Surveillance Conference ICNS '09*.
- [33] W. Glover, J. Lygeros, 2004, A stochastic hybrid model for air traffic control simulation, *Hybrid Systems: Computation and Control. Lecture Notes in Computer Science*, vol. 2993, pp. 372–386, 2004.
- [34] I. Lymperopoulos, J. Lygeros, 2010, Sequential Monte Carlo methods for multi-aircraft trajectory prediction in air traffic management, *International Journal of Adaptive Control and Signal Processing*, vol. 24, pp. 830–849.
- [35] J. Tenenbaum, L. Rukhovets, 2008, Determining biases in Hadley circulation reanalyses using independent aircraft observations, *Third WCRP International Conference on Reanalysis*, Tokyo.
- [36] zyGrib - GRIB File Viewer. Weather data visualization. <http://www.zygrib.org/>
- [37] C. Dey, 1998, GRIB (Edition 1) The WMO format for the storage of weather product information and the exchange of weather product messages in gridded binary form as used by NCEP central operations, U.S. Department of Commerce, National Oceanic and Atmospheric Administration, National Weather Service, National Centers for Environmental Prediction, office Note 388.
- [38] SourceForge.net. JGRIB. <http://jgrib.sourceforge.net/>
- [39] Current NAT tracks. http://aviation.allanville.com/nat_tracks/
- [40] North Atlantic tracker (NAT). Enroute Flightplanning Resource & Archive. <http://blackswan.ch/nat/>

Acknowledgements

The authors would like to thank Philippe Louyot for providing the real aircraft data files and the accompanying documents. The authors are also very grateful to Karim Legrand for productive discussions.

This work has been supported by French National Research Agency (ANR) through JCJC program (project ATOMIC n°ANR-12-JS02-009-01).

Email Addresses

Rodionova Olga: rodionova@recherche.enac.fr;

Daniel Delahaye: delahaye@recherche.enac.fr;

Mohamed Sbihi: sbihi@recherche.enac.fr;

Marcel Mongeau: mongeau@recherche.enac.fr

33rd Digital Avionics Systems Conference

October 5-9, 2014